

Enhanced Humoral Immune Response by High Density TLR Agonist Presentation on Hyperbranched Polymers

Celine S. Liong, Anton A. A. Smith, Joseph L. Mann, Gillie A. Roth, Emily C. Gale, Caitlin L. Maikawa, Ben S. Ou, and Eric. A. Appel*

Prophylactic vaccines often exploit adjuvants to drive potent and directed immune responses. Small-molecule toll-like receptor (TLR) agonists are promising adjuvant candidates; however, the poor pharmacokinetics and rapid distribution of these relatively hydrophilic small molecules results in systemic side effects that have limited their usage to topical application. In this study, TLR7/8 agonists are covalently attached to the highly dense end-groups of hyperbranched polymers synthesized by controlled radical polymerization techniques. Subcutaneous administration of these adjuvants results in a potent and prolonged type I interferon response. When co-administered in a model subunit vaccine, with ovalbumin or the HIV envelope glycoprotein gp120, these hyperbranched polymeric adjuvants potentiate an enhanced immunoglobulin response and near-immediate type-switching to IgG2c, suggesting they promote the type of strong T helper cell 1 immune response that is desirable for the treatment of intracellular pathogens such as mycobacterial and viral infections. Controlling the pharmacokinetics of potent TLR agonists through conjugation to hyperbranched polymers, therefore, enables the development of potent adjuvants in vaccines to drive durable and high-quality humoral immunity.

several TLR agonists have been discovered with high affinity for TLR7/8,^[2] endosomal receptors that detect viral ssRNA. TLR7/8 agonists (TLR7/8a) are designed to mimic genetic material in the cytoplasm resulting from viral infection and are attractive for vaccine development because they stimulate antigen presenting cells (APCs) to produce cytokines for a specific immune response (e.g., skewing Th response).^[3] Unfortunately, the pharmacokinetic profile of these compounds usually results in severe off-target toxicity and rapid systemic clearance.^[4] Consequently, the only clinically approved small-molecule TLR agonist is limited to topical application for treatment of viral infections and melanomas.^[4,5] The ability to control the pharmacokinetics of TLR7/8a would enable these highly potent agonists for broad use as vaccine adjuvants.^[6]


The conjugation of small molecule TLR7/8a to macromolecular constructs provides the ability to impede systemic clearance, positively affecting pharmacokinetic

profiles. Given that the TLR7/8's natural ligand is macromolecular cytoplasmic ssRNA, a polymeric presentation of synthetic TLR7/8a can also be expected to alter the pharmacodynamics in comparison to small molecule TLR7/8a. The most intensively studied macromolecular TLR7/8a constructs involve imidazoquinolines (IMQ) and their derivatives.^[7–11] The structure–function activity relationship for IMQ TLR7/8a has been mostly

profiles. Given that the TLR7/8's natural ligand is macromolecular cytoplasmic ssRNA, a polymeric presentation of synthetic TLR7/8a can also be expected to alter the pharmacodynamics in comparison to small molecule TLR7/8a. The most intensively studied macromolecular TLR7/8a constructs involve imidazoquinolines (IMQ) and their derivatives.^[7–11] The structure–function activity relationship for IMQ TLR7/8a has been mostly

C. S. Liong, Dr. G. A. Roth, C. L. Maikawa, B. S. Ou, Prof. E. A. Appel
Dept. of Bioengineering
Stanford University
Stanford, CA 94305, USA
E-mail: eappel@stanford.edu

Prof. A. A. A. Smith, J. L. Mann, Prof. E. A. Appel
Dept. of Materials Science & Engineering
Stanford University
Stanford, CA 94305, USA
Prof. A. A. A. Smith
Dept. of Chemistry
Aarhus University
Aarhus 8000, Denmark
E. C. Gale
Dept. of Biochemistry
Stanford University
Stanford, CA 94305, USA
Prof. E. A. Appel
ChEM-H Institute
Stanford University
Stanford, CA 94305, USA

 The ORCID identification number(s) for the author(s) of this article can be found under <https://doi.org/10.1002/adtp.202000081>

© 2021 The Authors. Advanced Therapeutics published by Wiley-VCH GmbH. This is an open access article under the terms of the Creative Commons Attribution-NonCommercial-NoDerivs License, which permits use and distribution in any medium, provided the original work is properly cited, the use is non-commercial and no modifications or adaptations are made.

DOI: 10.1002/adtp.202000081

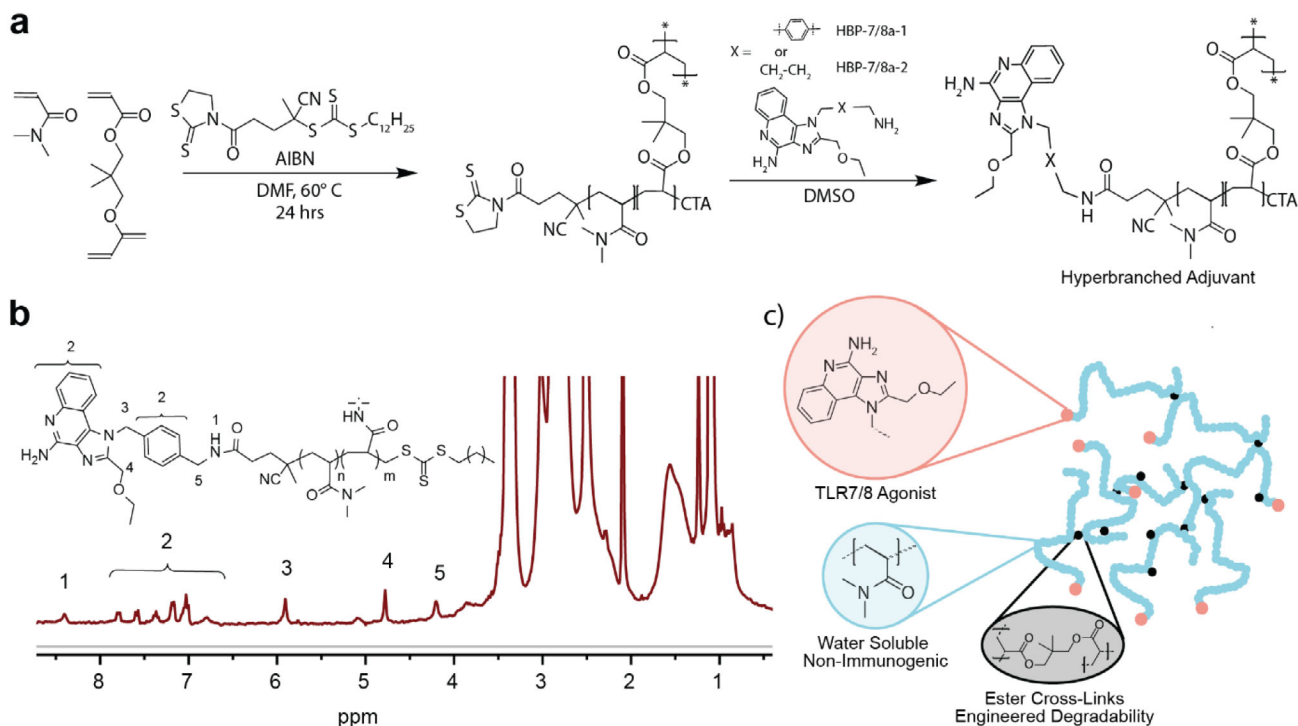


Figure 1. Design of hyperbranched TLR7/8 agonist (HBP-7/8a). a) Reversible addition fragmentation chain-transfer (RAFT) copolymerization of dimethyl acrylamide (DMA), neopentyl glycol diacrylate (NPGDA), and a 2-thiazolidinethione (TA) bearing chain transfer agent was followed by a fractional precipitation to remove low molecular weight polymeric species, and a post-fractional precipitation conjugation of an amine functionalized TLR7/8 agonist. b) ¹H NMR spectra of HBP-7/8a-1. c) Illustration of design features in HBP-7/8a.

elucidated, and analogues with ligation points that are non-detrimental to activity have been developed.^[12,13] The macromolecular constructs taking advantage of these have shown that systemic toxicity of IMQ can be reduced, while retaining efficacy as vaccine adjuvants.^[9] The potency of these constructs is significantly enhanced if they form a particle suspension, suggesting nanoscopic- to microscopic- presentation enhances the efficacy of TLR7/8a.^[7,8]

For this purpose, the hyperbranched polymer architecture is a promising delivery vehicle for TLR7/8a through its ability to alter the pharmacokinetics to simultaneously reduce systemic toxicity and increase targeted immune activation by introducing a high density of TLR7/8a moieties. Hyperbranched polymers can attain sizes relevant for lymphatic delivery, 10–100 nm in hydrodynamic radius, and masses in excess of 10 MDa, while still being unimolecular constructs with a globular architecture.^[14,15] Moreover, branched polymers have been found to be especially amenable to uptake in draining lymph nodes.^[16] As such, they present a size and shape regime that has not been explored for these purposes. In this work, we investigate a hyperbranched TLR7/8a adjuvant (HBP-7/8a) using controlled radical polymerization and post-polymerization functionalization. We explore how the macromolecular construct of HBP-7/8a alters pharmacodynamics by probing immune activation after intraperitoneal (IP) and subcutaneous (SC) injections. We subsequently investigate HBP-7/8a potential as an adjuvant in a subunit vaccine with ovalbumin as a model antigen and gp120 as a more clinically relevant antigen.

Hyperbranched polymers (HBPs) comprising poly(dimethylacrylamide) were synthesized by reversible addition fragmentation chain-transfer (RAFT) polymerization (Figure 1a). Poly(dimethylacrylamide) was selected for its water solubility and demonstrated biocompatibility.^[17,18] Neopentylglycol diacrylate was selected as the crosslinker for HBP synthesis such that the crosslinks in the high-molecular weight macromolecular construct bore esters susceptible to hydrolysis and enzymatic cleavage, yielding low molecular weight polymers amenable to renal clearance upon degradation in the body.^[19] The RAFT agent used carried a thiazolidine-2-thione (TA) on the R terminus, allowing facile conjugation by substrates bearing amines. High-molecular weight HBPs were recovered from this polymerization by fractional precipitation, resulting in lower dispersity HBP species amenable for conjugation of TLR7/8a moieties (Figures S2 and S3, Supporting Information).^[20] The polymer was subsequently functionalized with a parabenzyamine analog of R848 (TLR7/8a-1), a potent TLR7/8a, producing hypervalent TLR7/8a-1 presenting HBPs (HBP-7/8a-1). The syntheses of these constructs were confirmed by ¹H-NMR (Figure 1b). The design features and macromolecular construct is illustrated in Figure 1c. HBP-7/8a-1 exhibited relatively poor solubility in buffer at room temperature, likely arising from the high-density conjugation of the relatively hydrophobic TLR7/8a-1 moiety, but could nevertheless be dissolved completely by refrigeration overnight. Since polymer aggregation could potentially hinder reliable dosing and activity in vivo, HBP-7/8a-1 polymers were co-formulated with β -cyclodextrin, which served as a macrocyclic host to the

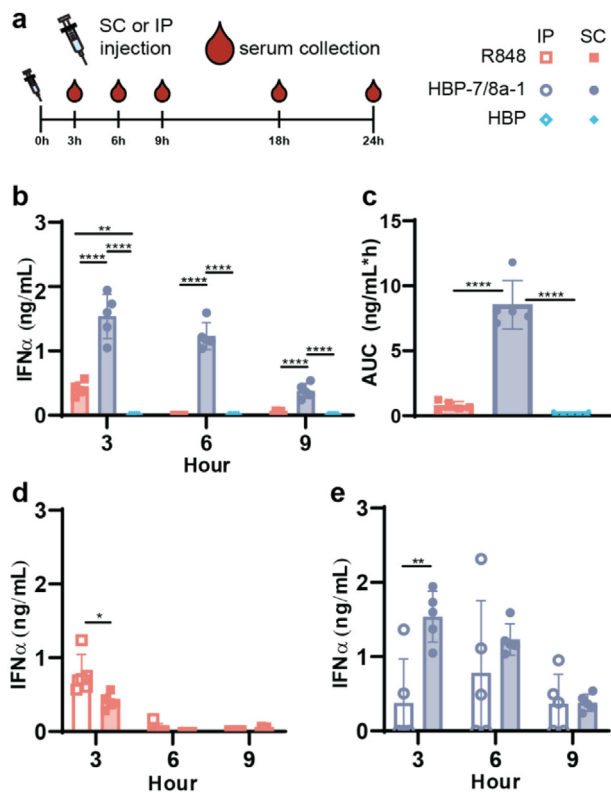


Figure 2. Conjugation of TLR7/8a-1 to hyperbranched polymer (HBP) increases and sustains immune activation. a) Study timeline of serum IFN α concentrations in C57BL/6 mice over 24 h following intraperitoneal (IP, hollow) or subcutaneous (SC, filled) administration of R848 (red), TLR7/8a-1 conjugated to hyperbranched polymer (HBP-7/8a-1, violet), or hyperbranched polymer control (HBP, blue). Statistical comparison of cytokine response between R848, HBP-7/8a-1, or HBP after b) SC administration and c) corresponding area under the curve. Statistical comparison of cytokine response between IP and SC injection for d) R848 and e) HBP-7/8a-1. For (b,c), all error bars are mean \pm s.d., $n=5$ per group ($n=4$ for HBP IP), $*p < 0.05$, $**p < 0.005$, $***p < 0.001$, $****p < 0.0001$, determined by one-way ANOVA with Tukey's post hoc test. Statistically significant comparisons from multiple comparisons are indicated. For (d,e), all error bars are mean \pm s.d., $n=5$ per group, $*p < 0.05$, $**p < 0.005$, determined by two-tailed t -test. Statistically significant comparisons are indicated.

TLR7/8a-1 moiety. The β -cyclodextrin binding to the TLR7/8a-1 enabled reliable solubilization of the HBP-7/8a-1 polymers in buffer.

To elucidate the possible adjuvant properties of HBP-7/8a-1, we measured the immune activation in response to R848, HBP-7/8a-1, and a hyperbranched polymer (HBP) negative control, following subcutaneous (SC) or intraperitoneal (IP) injection in C57BL/6 mice, with blood samples taken at regular intervals. When endocytosed, TLR7/8 activation results in type I interferons (IFN) such as IFN α . This ubiquitous mediator of immune responses is released in response pathogen-associated molecular patterns and is a reliable measure of inflammation.^[21] Conjugation of TLR7/8a-1 to the hyperbranched macromolecular construct extended the duration of IFN α production for both IP and SC administration when compared to R848 (Figure 2), which showed very short-lived IFN α production, regardless of in-

jection method, corroborating the relative short half-life of the small molecule adjuvant.^[7] HBP-7/8a-1 showed a significantly stronger and extended IFN α response, supporting the hypothesis that macromolecular conjugation alters the pharmacokinetics and biodistribution of the TLR7/8a-1. Dye-labeled HBP is present at the injection site up to 24 hours post injection (Figure S7a, Supporting Information). No IFN α production was detected when HBP was injected either intraperitoneally (IP) or subcutaneously (SC), indicating the HBP is non-immunogenic by itself, in the absence of conjugated TLR7/8a-1. The increased cytokine production observed with HBP-7/8a-1, therefore, is a result of the altered pharmacokinetics of the conjugated TLR7/8a-1 moiety rather than any inherent adjuvant properties of the polymer construct.

The effects of the macromolecular conjugation was more pronounced after SC injection (Figure 2b,c). The cytokine production following R848 administration SC was relatively short-lived, whereby IFN α concentrations dropped to almost undetectable levels by 3 h following administration. Comparatively, HBP-7/8a-1 administration SC resulted in sustained immune activation for up to 18 h after administration (Figure S6, Supporting Information). Moreover, administration of HBP-7/8a-1 increased the cumulative concentration of IFN α by almost an order of magnitude in comparison to the small molecule R848. Because HBP-7/8a-1 has a hydrodynamic radius of 15 nm (Figure S1, Supporting Information), it is too large to enter circulation directly from the SC space. The elimination of the HBP-7/8a-1 species requires passing through the lymphatic system, resulting in an increased exposure at the injection site and the draining lymph nodes.^[15] Lymphatic trafficking is corroborated by dye-labeled HBP seen in the draining lymph node 3 hours post injection (Figure S7c, Supporting Information). The increased residence time and exposure to APCs likely elicits a stronger immune response and consequently higher IFN α concentrations over prolonged timeframes. This response will likely be stronger in other models as TLR 8 agonism is hypothesized to inhibit effects of TLR 7 activation in mice, and mice are likely to have a comparatively weaker response.^[22]

The route of administration also influenced the severity of immune activation (Figure 2d,e). R848 exhibited higher immune activation following IP administration because of the faster absorption compared to SC. Yet, as it is also eliminated rapidly, there was no observable difference in IFN α production between the two routes of administration after 6 hours. In contrast, the response from the IP administration of HBP-7/8a-1 was weaker and shorter lived than SC administration. We hypothesize that a longer residence time at the site of injection following SC administration gives rise to this observation of more potent and durable IFN α production.

As shown in the work by Lynn et. al., submicron particles presenting TLR7/8a elicit stronger type I interferon responses.^[8] This effect is likely not present when HBP-7/8a-1 is administered IP due to the larger immediate volume of distribution in this space and more rapid clearance. Moreover, there may be more cell types with higher TLR7/8 expression near the SC injection site due to its proximity to the skin, where there are higher dendritic cell populations. As more cells may be activated at the SC injection site, HBP-7/8a-1 SC administration may lead to higher cytokine production.

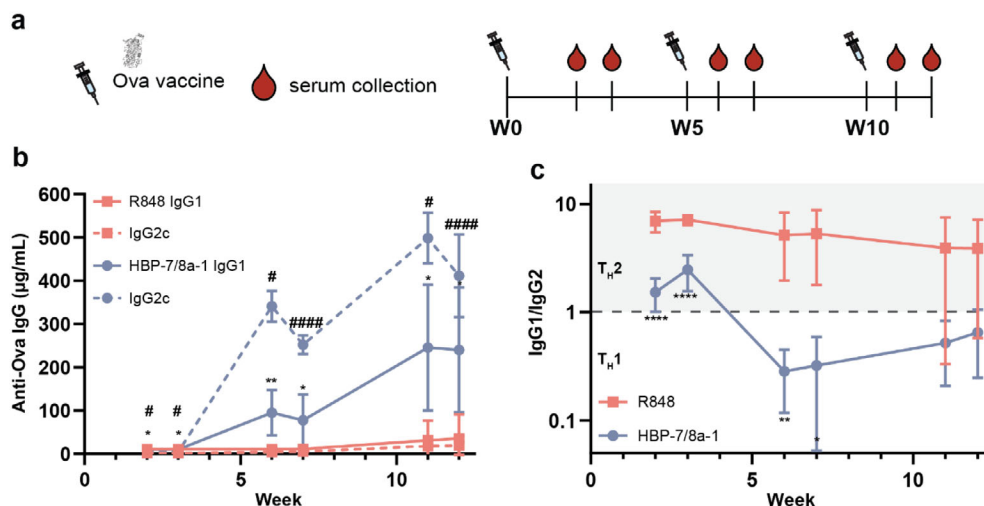


Figure 3. HBP-7/8a-1 adjuvants increase anti-Ova antibody responses and skew T helper cell (Th) response in model subunit vaccines. a) Study timeline of subcutaneous administration of prime (week 0) and boost (week 5 and 10) vaccines comprising Ova (100 µg) and either R848 or HBP-7/8a-1 adjuvants (1 mg, 50 µg TLR7/8a equivalent). b) Anti-Ova IgG1 (solid) and IgG2c (dashed) concentrations during vaccine study with R848 (red) or HBP-7/8a-1 (violet) as adjuvant. c) Ratio of IgG1 to IgG2c isotypes, indicating skew to type 1 or 2 Th responses. All error bars are mean \pm s.d., $n=5$ per group. * $p < 0.05$, ** $p < 0.005$, *** $p < 0.0001$ for IgG1 comparisons and # $p < 0.05$, ### $p < 0.0001$ for IgG2c comparisons, determined by two-tailed t -test. Statistically significant comparisons are indicated.

Overall, the stronger immune activation observed for the HBP-7/8a-1 species when compared with the R848 would be expected to translate into more potent and durable antibody responses against a co-presented antigen when used as adjuvants in vaccines. C57BL/6 mice were administered with subunit vaccines comprising ovalbumin (Ova; 100 µg) and either R848 or HBP-7/8a-1 adjuvants in doses established efficacious in previous studies (50 µg total dose of TLR7/8a).^[7–10,17] R848 induced only a modest IgG response, primarily consisting of IgG1 (Figure 3a,b). As expected, IgG antibodies increased with each vaccine dose, with the increase following the boost observed to be more drastic with the HBP-7/8a-1 adjuvanted vaccine. The comparatively large increases are likely due to APC uptake of the HBP-7/8a-1 and effective lymph node drainage, which can prolong antigen presentation in germinal centers.

Previous work has seen that 30 nm particles are optimal for APC uptake and presentation.^[23] Additionally, macromolecular constructs of TLR7/8a moieties have previously been shown to exhibit longer lymph node residence time than their small molecule counterparts.^[8,17] Likely due to a longer residence time, HBP-7/8a-1 constructs induced significantly earlier seroconversion than the small molecule counterpart, producing antibodies of the IgG2c immunoglobulin subclass rather than the IgG1 subclass. This IgG subclass skew increases following the vaccine boost, consistent with previous findings that conjugating TLR7/8a to a polymeric construct can modulate the Th response.^[8] Isotype switching to IgG2c signifies an immediate skew to a T helper cell 1 (Th1) response to the antigen, with one mouse that received the HBP-7/8a-1 adjuvanted vaccine not producing any IgG1 antibodies at all, but rather exhibiting a strong IgG2c response. A Th1 type cytokine response is associated with an increased and sustained cell-mediated immune response against cancers and intracellular pathogens, such as parasites and viruses.^[24,25] To elicit a Th1 response against viral antigens,

it is often necessary to use live-attenuated vaccines, or antigens conjugated to TLR agonists.^[25,26]

To test an antigen with less inherent immunogenicity, C57BL/6 mice were administered with subunit vaccines comprising the HIV envelope glycoprotein gp120 (20 µg) and either a small molecule TLR7/8a (an alternative shown in Figure 1a and denoted TLR7/8a-2) delivered alongside HBP or covalently conjugated to the HBP (HBP-7/8a-2). Similar to the Ova vaccines described above, the IgG2c antibody titers are significantly higher in mice receiving vaccines with HBP-7/8a-2 compared to those receiving the physical mixture of HBP and the small molecule TLR7/8a-2 (Figure 4d) or R848 (Figure S8, Supporting Information). The adjuvant's prolonged residence time arising from conjugation to the HBP likely facilitates improved lymph node trafficking and the multivalent HBP presentation of the adjuvant likely increases APC uptake.

While non-covalent interactions between the adjuvant and HBP are possible, they do not sufficiently alter the pharmacokinetics or biodistribution of the adjuvant molecules to elicit the potent Th1 skew observed for vaccines comprising HBP-7/8a-2. While a stronger Th1 response is observed with vaccines comprising HBP-7/8a-2, no difference in IgG1 titers, an indicator of Th2 responses, was observed when mice were immunized with gp120 and small molecule adjuvants. These responses contrast with the Ova vaccines described above, which may have elicited a Th2 skewed response due to the antigen's own immunogenicity, which has been shown to elicit Th2 skewed responses.^[27] Regardless of antigen, HBP conjugation of potent TLR7/8 agonists induces potent Th1 responses for a targeted immune signature, which is particularly important for vaccines combating viral pathogens.

Based on the enhanced potency of the HBP-7/8a-2 adjuvant construct, we then evaluated the potential for adjuvant dose sparing. Indeed, a 10 µg dose of HBP-7/8a-2 dose was observed to

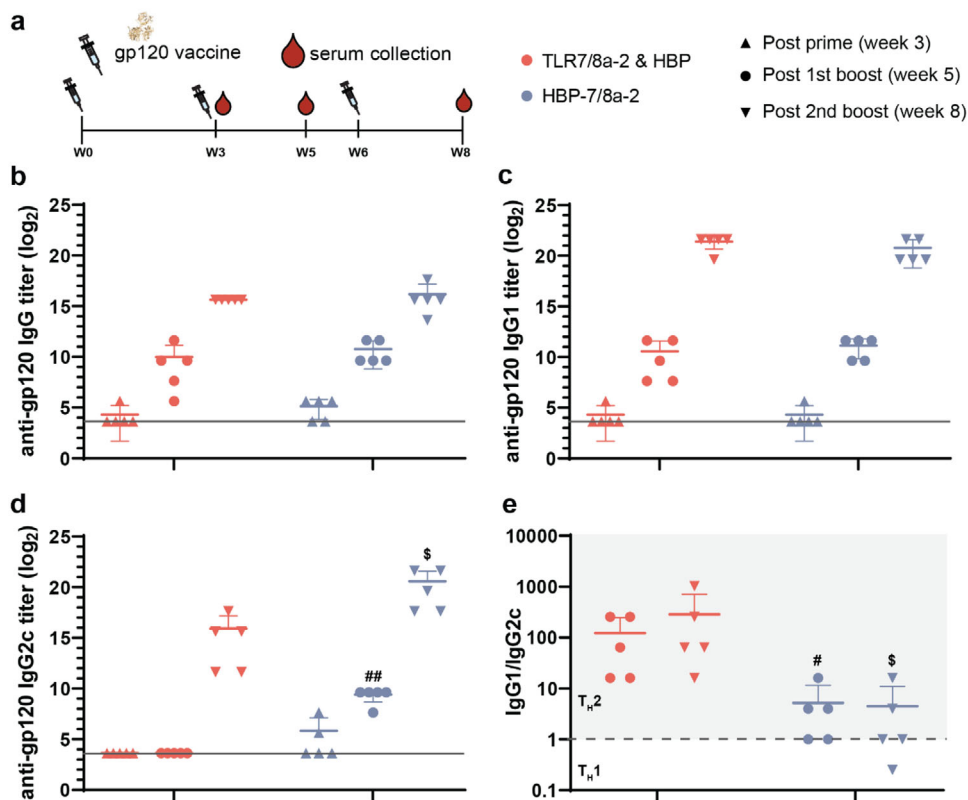


Figure 4. HBP-7/8-2 adjuvants elicit more potent anti-gp120 responses and induce Th1 skew with HIV-targeted subunit vaccines. a) Study timeline of subcutaneous administration of prime (week 0) and boost (week 3 and 6) vaccines comprising gp120 (20 μ g) and either TLR7/8a-2 or HBP-7/8a-2 as adjuvants (1 mg, 50 μ g TLR7/8a equivalent). b) Total IgG endpoint titers, c) IgG1 endpoint titers, and d) IgG2c endpoint titers post prime and post boosts (week 3, 5, and 8). e) IgG1/IgG2c ratio indicating Th2 and Th1 skew, respectively, at week 5 and 8. All error bars are mean \pm s.d., $n=5$ per group. # $p < 0.05$, ## $p < 0.005$ for week 5, and \$ $p < 0.05$ for week 8, determined by REML mixed model with two tailed t -test. Statistically significant comparisons from multiple comparisons are indicated.

elicit equivalent IgG2c titers and Th1 skew to that of the control vaccine comprising a 50 μ g dose of the small molecule TLR7/8a-2 and HBP (Figure S9, Supporting Information). While the HBP-TLR7/8a-2 constructs enhanced vaccine efficacy and can significantly reduce the adjuvant dosing needed to match the efficacy of vaccines comprising the small molecule TLR7/8a-2, dose matching was needed to induce higher antibody titers and more potent Th1 skew to increase vaccine efficacy. The multivalent presentation of TLR7/8a adjuvants on the HBP construct offers a favorable immune response that is otherwise difficult to achieve with subunit vaccines comprising standard small molecule adjuvants.

Altogether, the findings indicate that high density presentation of TLR7/8 agonists on macromolecular constructs such as HBP-7/8a promotes a potent cell-mediated immune response against a co-presented antigen when compared to the small molecule TLR7/8 agonist itself. This effect likely arises from enhanced pharmacokinetics and better lymph node draining, favoring presentation to dendritic cells mediating the response, on account of the hydrodynamic size of these macromolecular species. These HBP-7/8a adjuvants have implications for the development of vaccines for intracellular pathogens, such as viral infections and mycobacterial infections, as they drive potent and durable type I interferon responses, and result in rapid antibody isotype switching to the favorable IgG2c immunoglobulin subclass.^[28] Control-

ling the pharmacokinetics of potent TLR7/8 agonists through conjugation to hyperbranched polymers, therefore, enables the development of potent adjuvants in vaccines to drive durable and high-quality humoral immunity.

Experimental Section

HBP Synthesis: TA-CTA was synthesized as described in literature.^[29] DMA-co-NPGDA branched polymer targeting a CTA:Crosslinker ratio of 1.4:1 and a CTA:Monomer of 50 was as follows. DMA (10 g, 100.9 mmol, filtered through basic alumina), NPGDA (0.60 mg, 2.8 mmol), TA-CTA (1.02 g, 2.01 mmol), and AIBN (66 μ g, 0.4 mmol) were diluted with DMF to a total volume of 25 mL ([DMA] = 4M). The solution was divided into two 20 mL scintillation vials equipped with a PTFE septa. The reaction mixture was sparged with nitrogen for 15 min and heated to 65 $^{\circ}$ C for 12 h. Following polymerization, the reaction mixture was precipitated into ether and dried under vacuum. The resulting polymer was dissolved into dioxane (10 w/v%). Under vigorous stirring, ether was added until the solution became opaque. The opaque solution was centrifuged and decanted. The remaining high molecular weight polymer was precipitated into ether. A monomer conversion of 94% was calculated from the unreacted vinyl peaks ($\delta = 5.6$ ppm, 1H) and polymeric backbone ($\delta = 5.6$ ppm, 6H) of the post polymerization reaction mixture using 1 H NMR. The fractional precipitation reduced the wt% of unincorporated primary chains from approximately 35 to 9 wt% (determined through SEC analysis in DMF; see Figure S2, Supporting Information). Different scales of

synthesis and fractional precipitation can yield different molecular weights and sizes of the hyperbranched polymer. M_n , \bar{D} , and R_g for HBP used in the ovalbumin vaccination (HBP-7/8a-1) were determined as 445 kDa, 2.0, and 17 nm, respectively, by SEC-MALLS in THF using a dn/dc value of 0.11 mL g^{-1} as determined through serial batch injections of varying polymer concentrations. M_n , \bar{D} , and R_g for HBP used in the gp120 vaccination (HBP-7/8a-2) were determined as 101 kDa, 2.4, and 14 nm, respectively, by SEC-MALLS in THF. R_n and polydispersity of 22.6 and 0.2 nm for HBP used in the GP120 vaccination were determined in MilliQ water through DLS.

HBP-7/8a-1 Synthesis for Ovalbumin Vaccination: (1-(4-(aminomethyl)benzyl)-2-(ethoxymethyl)-1H-imidazo[4,5-c]quinolin-4-amine) TLR agonist (TLR7/8a-1) was synthesized as described previously.^[30] HBP post fractional precipitation (100 mg) was dissolved in 1 mL of DMSO. 1.05 equiv. of TLR agonist was added with respect to TA groups (7.6 mg, 21 μmol) and the solution was incubated at room temperature for 5 h. DMSO was removed by repeated extraction with diethyl ether, retaining two phases throughout the procedure, until light yellow powder was obtained. This was further triturated with diethyl ether to remove any residual DMSO, followed by drying *in vacuo*. For dissolution prior to injection, the compound was dissolved overnight at 5°C in PBS at 20 mg mL^{-1} , in the presence of 10 mg mL^{-1} β -CD.

HBP-Dye Synthesis: HBP-TA (7 mg; 1 equiv.) was dissolved in DMSO (100 μL). Cyanine5-amine (0.135 mg; 0.15 eq) dissolved in of DMSO (27 μL) was added to the solution, which was vortexed and left at room temperature for 1 h. Butylamine (0.102 mg, 1 equiv.) dissolved in DMSO (10 μL) was then added to the reaction solution, which was vortexed and left at room temperature for 1 h. The HBP-dye was purified by passing through PD MiniTrap G-10 desalting column (700 M_r, milliQ water eluent, 2.1 mL collection). Dye concentration was determined by SEC-UV-vis analysis (Figure S5, Supporting Information) whereby 30 μL of the collection solution was diluted into DMF (1 mL) and the area under the curve of the absorbance at 650 nm (AUC_{650}) was compared to AUC_{650} of a 5 mg mL^{-1} stock solution of cyanine5-amine in DMSO (diluted an additional 20 μL of stock solution in 1 mL DMF).

HBP-7/8a-2 Synthesis for gp120 Vaccination: HBP-TA (50 mg, 1 eq) was dissolved in DMSO (150 μL). TLR7/8a-2 (3.8 mg, 1.3 equiv.) (Career Henan Chemical Corp, 4-amino-2-(ethoxymethyl)-1H-imidazo[4,5-c]quinoline-1-butanamine, CAS number 210304-20-4) dissolved in DMSO (150 μL) was added to the solution, which was vortexed and left at room temperature for 1 h. The reaction was precipitated twice from ether, yielding flaky off-white polymer. Conjugation was confirmed via a disappearance of the amide protons at 4.5 ppm (DMSO- d_6 , ^1H NMR), presence of aromatic protons (8–7 ppm, DMSO- d_6 , ^1H NMR, Figure S4, Supporting Information), and an increase in the UV (330, 250) to RI ratio after SEC analysis.

HBP-butylamine Synthesis for gp120 Vaccination: HBP-TA (80 mg, 1 equiv.) was dissolved in DMSO (400 μL). Butylamine (1.18 mg, 1 equiv.) in DMSO (133 μL) was added to the solution, which was vortexed and left at room temperature for 1 h. The reaction was precipitated twice from ether, yielding flaky off-white polymer. TA group cleavage confirmed by disappearance of amide protons at 4.5 ppm (DMSO- d_6 , ^1H NMR).

Animal Studies: 7–8 weeks old female C57BL/6 mice were obtained from Charles River and were cared for according to Institutional Animal Care and Use guidelines. Animal studies were performed in accordance with the guidelines for the care and use of laboratory animals. Protocol #32 109 was approved by the Stanford Institutional Animal Care and Use Committee.

In Vivo IFN α Quantification: Mice were injected, subcutaneously or intraperitoneally, with phosphate buffered saline (PBS) (100 μL) with 50 μg TLR7/8 agonist and 100 μg ovalbumin. Serum was collected via tail vein blood collection. IP serum samples were diluted 1:100 and SC samples were diluted 1:50. IFN α levels were quantified by ELISA according to manufacturer's instructions (PBL Assay Science). Absorbance was measured at 450 nm in a Synergy H1 Microplate Reader (BioTek). Concentrations were calculated based on standard curves which were determined via logarithmic interpolation of the 450 nm absorbance values and a seven stage series 1:1 dilution series.

Whole Animal Imaging: Biodistribution and pharmacokinetics of Cy5-labeled HBP was evaluated via IVIS imaging (Perkin Elmer Lumina III). Mice were injected subcutaneously with dye-labeled HBP and imaged at serial time points of 0, 3, 6, and 24 h post-injection (excitation of 700 nm and emission of 760 nm). The signal was quantified within a region of interest by Aura Imaging Software (Spectral Instruments Imaging).

Vaccine Study: C57BL/6 (B6) mice from Charles River were subcutaneously injected with a 100 μL PBS bolus while mice were administered isoflurane anesthesia. Injections were done with a 26-gauge needle. Serum was collected via tail vein blood collection for survival studies and cardiac puncture for terminal studies. The gp120 vaccine study was designed as random block design with cage as a blocking factor; each vaccine formulation was represented once within each cage. Mice were randomly assigned to a treatment within each cage.

Anti-Ova IgG Antibody Quantification: For IgG1 quantification, serum was diluted 1:2000. The anti-OVA IgG1 ELISA (Cayman Chemicals) was performed per manufacturer's instructions. Absorbance was measured at 405 nm with a Synergy H1 Microplate Reader (BioTek). Antibody concentrations were calculated based on standard curves. IgG2c quantification was determined with anti-OVA IgG2c ELISA (Chondrex) per manufacturer's instructions. R848 samples were diluted 1:2000. HBP-7/8a samples were diluted 1:2000 for post-prime samples and 1:200 000 for post-boost samples. Absorbance was measured at 405 nm with a Synergy H1 Microplate Reader (BioTek). Antibody concentrations were calculated based on standard curves determined by a quadratic fit between the 450 nm absorbance values and a seven stage 1:1 dilution series.

Anti-gp120 IgG Endpoint Titers: Serum was diluted with 1% BSA starting at 1:50 in a seven stage 1:4 dilution series. 96-well half area plates were incubated with 2.5 $\mu\text{g mL}^{-1}$ gp120 in PBS overnight at 4 °C. Plates were then blocked with 1% BSA for 1 h at room temperature. Serum was incubated for 2 h at room temperature. Secondary antibodies were diluted 1:10000 and incubated for 1 h at room temperature. Plates were developed in TMB until an OD reading of 0.5 at 650 nm and stopped with 1 N HCl. Plates were read at 450 nm for endpoint titers, defined as the highest dilution with an OD above 0.1. Plates were washed five times with 0.05% Tween 20 in PBS between all incubation steps.

Statistical Analysis: All error bars are mean \pm S.D. Sample size of $n = 5$ per group, apart from the HBP IP injection and HBP-7/8a-2 2 μg group with $n = 4$. Probability (p) values are denoted as * $p < 0.05$, ** $p < 0.005$, *** $p < 0.001$, and **** $p < 0.0001$. For IFN α and anti-Ova IgG concentrations, p -values were determined by one-way ANOVA with Tukey's post hoc test or two tailed t-test. All statistical analysis was performed in GraphPad Prism. For anti-gp120 endpoint titers, analysis was performed in JMP Pro 14. Endpoint titers required additional transformation using log base 2 to meet assumptions of homoscedasticity. A restricted maximum likelihood (REML) mixed model was used with a Tukey's post hoc test or two tailed t-test. The mouse was included as a random effect subject. Cage was included as a fixed effect blocking (control) factor to account for variation in response between cages.

Supporting Information

Supporting Information is available from the Wiley Online Library or from the author.

Acknowledgements

C.S.L. and A.A.A.S. contributed equally to this work. A.A.A.S. is supported by the Novo Nordisk Foundation and the Stanford Bio-X Program, NNF18OC0030896. C.S.L. and J.L.M. are supported by the National Defense Science & Engineering Graduate (NDSEG) Fellowship. J.L.M. is supported by the Stanford Graduate Fellowship. B.S.O. is supported by the Eastman Kodak Fellowship. This research was financially supported by the Center for Human Systems Immunology with the Bill and Melinda Gates Foundation (OPP1113682).

Conflict of Interest

The authors declare no conflict of interest.

Data Availability Statement

All data supporting the results in this study are available within the Article and its Supplementary Information. The broad range of raw datasets acquired and analyzed (or any subsets of it), which for reuse would require contextual metadata, are available from the corresponding author on reasonable request.

Keywords

adjuvants, drug delivery, immunoengineering, polymers, vaccines

Received: April 17, 2020
Revised: January 16, 2021
Published online:

-
- [1] M. Singh, D. O'Hagan, *Nat. Biotechnol.* **1999**, *17*, 1075.
- [2] C. E. Schiaffo, C. Shi, Z. M. Xiong, M. Olin, J. R. Ohlfest, C. C. Aldrich, D. M. Ferguson, *J. Med. Chem.* **2014**, *57*, 339.
- [3] D. S. Green, A. G. Dalgleish, N. Belonwu, M. D. Fischer, M. D. Bodman-Smith, *Br. J. Dermatol.* **2008**, *159*, 606.
- [4] A. L. Engel, G. E. Holt, H. Lu, *Expert Rev. Clin. Pharmacol.* **2011**, *4*, 275.
- [5] C. Shi, Z. M. Xiong, P. Chittepudi, C. C. Aldrich, J. R. Ohlfest, D. M. Ferguson, *ACS Med. Chem. Lett.* **2012**, *3*, 501.
- [6] D. J. Dowling, *Immunohorizons* **2018**, *2*, 185.
- [7] G. M. Lynn, P. Chytil, J. R. Francica, A. Lagova, G. Kueberuwa, A. S. Ishizuka, N. Zaidi, R. A. Ramirez-Valdez, N. J. Blobel, F. Baharom, J. Leal, A. Q. Wang, M. Y. Gerner, T. Etrych, K. Ulbrich, L. W. Seymour, R. A. Seder, R. Laga, *Biomacromolecules* **2019**, *20*, 854.
- [8] G. M. Lynn, R. Laga, P. A. Darrah, A. S. Ishizuka, A. J. Balaci, A. E. Dulcey, M. Pechar, R. Pola, M. Y. Gerner, A. Yamamoto, C. R. Buechler, K. M. Quinn, M. G. Smelkinson, O. Vanek, R. Cawood, T. Hills, O. Vasalatiy, K. Kastenmuller, J. R. Francica, L. Stutts, J. K. Tom, K. A. Ryu, A. P. Esser-Kahn, T. Etrych, K. D. Fisher, L. W. Seymour, R. A. Seder, *Nat. Biotechnol.* **2015**, *33*, 1201.
- [9] L. Nuhn, S. De Koker, S. Van Lint, Z. Zhong, J. P. Catani, F. Combes, K. Deswarte, Y. Li, B. N. Lambrecht, S. Lienenklaus, N. N. Sanders, S. A. David, J. Tavernier, B. G. De Geest, *Adv. Mater.* **2018**, *30*, 1803397.
- [10] L. Nuhn, L. Van Hoecke, K. Deswarte, B. Schepens, Y. Li, B. N. Lambrecht, S. De Koker, S. A. David, X. Saelens, B. G. De Geest, *Biomaterials* **2018**, *178*, 643.
- [11] D. S. Wilson, S. Hirose, M. M. Raczky, L. Bonilla-Ramirez, L. Jeanbart, R. Wang, M. Kwissa, J. F. Franetich, M. A. S. Broggi, G. Diaceri, X. Quaglia-Thermes, D. Mazier, M. A. Swartz, J. A. Hubbell, *Nat. Mater.* **2019**, *18*, 175.
- [12] N. M. Shukla, S. S. Malladi, C. A. Mutz, R. Balakrishna, S. A. David, *J. Med. Chem.* **2010**, *53*, 4450.
- [13] W. G. Kim, B. Choi, H.-J. Yang, J.-A. Han, H. Jung, H. Cho, S. Kang, S. Y. Hong, *Bioconjugate Chem.* **2016**, *27*, 2007.
- [14] J. L. Mann, R. L. Rossi, A. A. A. Smith, E. A. Appel, *Macromolecules* **2019**, *52*, 9456.
- [15] A. Schudel, D. M. Francis, S. N. Thomas, *Nat. Rev. Mater.* **2019**, *4*, 415.
- [16] T. R. Bagby, S. F. Duan, S. Cai, Q. H. Yang, S. Thati, C. Berkland, D. J. Aires, M. L. Forrest, *Eur. J. Pharm. Sci.* **2012**, *47*, 287.
- [17] S. Van Herck, K. Deswarte, L. Nuhn, Z. Zhong, J. P. Portela Catani, Y. Li, N. N. Sanders, S. Lienenklaus, S. De Koker, B. N. Lambrecht, S. A. David, B. G. De Geest, *J. Am. Chem. Soc.* **2018**, *140*, 14300.
- [18] P. H. Kierstead, H. Okochi, V. J. Venditto, T. C. Chuong, S. Kivimaa, J. M. J. Fréchet, F. C. Szoka, *J. Controlled Release* **2015**, *213*, 1.
- [19] M. E. Fox, F. C. Szoka, J. M. J. Fréchet, *Acc. Chem. Res.* **2009**, *42*, 1141.
- [20] J. L. Mann, A. K. Grosskopf, A. A. A. Smith, E. A. Appel, *Biomacromolecules* **2020**, *21*, 3704.
- [21] O. Demaria, P. P. Pagni, S. Traub, A. de Gassart, N. Branzk, A. J. Murphy, D. M. Valenzuela, G. D. Yancopoulos, R. A. Flavell, L. Alexopoulos, *J. Clin. Invest.* **2010**, *120*, 3651.
- [22] F. McNab, K. Mayer-Barber, A. Sher, A. Wack, A. O'Garra, *Nat. Rev. Immunol.* **2015**, *15*, 87.
- [23] S. N. Thomas, E. Vokali, A. W. Lund, J. A. Hubbell, M. A. Swartz, *Biomaterials* **2014**, *35*, 814.
- [24] a) L. Stobie, S. Gurunathan, C. Prussin, D. L. Sacks, N. Glaichenhaus, C.-Y. Wu, R. A. Seder, *Proc. Natl. Acad. Sci. USA* **2000**, *97*, 8427; b) M. L. Disis, W. C. Watt, D. L. Cecil, *Oncol Immunology* **2014**, *3*, 8427.
- [25] S. Garlapati, *Expert Rev. Vaccines* **2012**, *11*, 1307.
- [26] U. Wille-Reece, B. J. Flynn, K. Loré, R. A. Koup, R. M. Kedl, J. J. Maitland, W. R. Weiss, M. Roederer, R. A. Seder, *Proc. Natl. Acad. Sci. USA* **2005**, *102*, 15190.
- [27] a) R. Roy, S. Kumar, A. K. Verma, A. Sharma, B. P. Chaudhari, A. Tripathi, M. Das, P. D. Dwivedi, *Int. Immunol.* **2014**, *26*, 159; b) M. Ban, I. Langonné, N. Hugué, Y. Guichard, M. Goutet, *Toxicol. Lett.* **2013**, *216*, 31; c) C. A. Herrick, H. MacLeod, E. Glusac, R. E. Tigelaar, K. Bottomly, *J. Clin. Invest.* **2000**, *105*, 765.
- [28] a) I. A. Ramshaw, A. J. Ramsay, G. Karupiah, M. S. Rolph, S. Mahalingam, J. C. Ruby, *Immunol Rev.* **1997**, *159*, 119; b) I. Smith, *Clin. Microbiol. Rev.* **2003**, *16*, 463; c) A. Mantovani, P. Allavena, A. Sica, F. Balkwill, *Nature* **2008**, *454*, 436.
- [29] A. A. A. Smith, K. Zuwala, O. Pilgram, K. S. Johansen, M. Tolstrup, F. Dagnaes-Hansen, A. N. Zelikin, *ACS Macro Lett.* **2016**, *5*, 1089.
- [30] A. A. A. Smith, E. C. Gale, G. A. Roth, C. L. Maikawa, S. Correa, A. C. Yu, E. A. Appel, *Biomacromolecules* **2020**, *21*, 3704.